



Screen-printed Carbon Electrode from Coconut Shell Activated Carbon Modified with Ferrocene for Cobalt Detection

Muhammad Farhan^{a,b}, Eddy Herald^{a,b}, Abu Masykur^{a,c}, Muhammad A. Munir^d, Fitriah Rahmawati^{a,b*}

^aDepartment of Chemistry, Faculty of Mathematics and Natural Sciences, Sebelas Maret University
Jalan Ir. Sutami 36 A, Kentingan, Surakarta, 57126, Indonesia

^bResearch Group of Solid-State Chemistry & Catalysis, Department of Chemistry, Sebelas Maret University,
Jalan Ir. Sutami 36 A, Kentingan, Surakarta, 57126, Indonesia

^cResearch Group of Analytical and Environmental Science, Department of Chemistry, Sebelas Maret University,
Jalan Ir. Sutami 36 A, Kentingan, Surakarta, 57126, Indonesia

^dFaculty of Resource Science and Technology, University Malaysia Sarawak,
Kota Samarahan, 94300, Malaysia

*Corresponding author: fitriah@mipa.uns.ac.id

DOI: 10.20961/alchemy.20.2.81386.247-256.

Received 8 December 2023, Revised 28 May 2024, Accepted 18 August 2024, Published 30 September 2024

Keywords:

carbon;
coconut shell;
electrode for
analysis;
screen-printed
carbon electrode.

ABSTRACT. This research aims to fabricate a screen-printed carbon electrode (SPCE) from coconut shell charcoal. The charcoal was activated with NaOH to produce activated carbon (Ac). It was mixed with acetylene black (AB) and poly (vinylidene) Fluoride (PVDF) at the mass ratio of 7:2:1 for the Ac, AB, and PVDF, respectively, followed by a dispersing with N-Methyl-2-Pyrrolidinone (NMP) producing carbon slurry that was painted on a SPCE template. To increase electrochemical sensitivity, ferrocene, Fc was dropped onto the working electrode part at 10%, 20%, and 30% of the total SPCE mass. The results show that Ac is amorphous with a porous chip-like morphology containing 61.7% carbon. Ac shows vibrations of O–H, C=O, C=C, C–O, and Si–O with surface area and average pore size of 154.612 m² g⁻¹ and 1.42 nm, respectively. The cyclic voltammetry analysis found that 10% Fc on SPCE provides the highest current density compared to 20% and 30%. Meanwhile, the 2 mV s⁻¹ scanning rate reveals a more defined anodic and cathodic peak than 3 mV s⁻¹ and 5 mV s⁻¹. Furthermore, the SPCE with 10% Fc shows a good sensitivity to Co (II) ions, proven by a low detection limit (LoD) of 0.224 mmol L⁻¹.

INTRODUCTION

The oil production needs over 3 million tons of coconut annually. Coconut shells are one of the solid wastes produced from this production (Trisunaryanti *et al.*, 2022). Coconut shell mainly consists of carbon elements due to its cellulose (36%), hemicellulose (25%), and lignin (28%) content (Kuan-Ching *et al.*, 2021). The high carbon content in coconut shells makes them a potential raw material for producing activated carbon (Sujiono *et al.*, 2022). In addition, coconut shells have other advantages, such as their low cost and renewability. The sustainability of raw materials is important once mass production is projected. Because carbon is essential for some applications, including adsorption, vapor adsorption (Ridassepri *et al.*, 2020), photocatalyst support (Rahmawati *et al.*, 2017), water electrode materials, photoelectrodes, and methylene blue adsorption (Rahmawati *et al.*, 2023). Carbon is also the main component of analytical electrodes. Despite carbon produced from coal, recently, carbon derived from biomass has been studied for electrode fabrication such as screen-printed carbon electrode (SPCE) which was fabricated from sugarcane carbon for Cu²⁺ analysis (Rahmawati *et al.*, 2023), carbonized-waste paper pulp for a nanocarbon-supported NiFe₂O₄ electrode for clenbuterol analysis (Ma *et al.*, 2022), and SPCE from nano biochar for nitrites analysis in water (Ferlazzo *et al.*, 2023).

Activation is an important step in carbon preparation to increase carbon performance, especially the surface area. A high surface area of carbon is required for electrode preparation because a high surface area indicates a large reaction scene for electrochemical reactions on the carbon surface. Activation also removes silicate, which

Cite this as: Muhammad, F., Herald, E., Masykur, A., Munir, M. A. and Rahmawati, F., 2024. Screen-Printed Carbon Electrode from Coconut Shell Activated Carbon Modified with Ferrocene for Cobalt Detection *ALCHEMY Jurnal Penelitian Kimia*, 20(2), 247–256 . <https://dx.doi.org/10.20961/alchemy.20.2.81386.247-256>.

is naturally available in biomass. The presence of silicate influences the electrode performance due to its resistive properties and prevents mesopore formation (Rahmawati *et al.*, 2023).

Some modifications can simply be applied to SPCE to increase the selectivity and sensitivity, such as by applying ferrocene (Fc) to SPCE for Cu²⁺ analysis by electrochemical voltammetric method (Rahmawati *et al.*, 2023; Wu *et al.*, 2022). Ferrocenium complex is a strong oxidant that can increase electrochemical reactions on the working electrode's surface (Hu *et al.*, 2018). The Interaction of Fc and carbon can increase their electrocatalytic activity and accelerate electron movement (Wu *et al.*, 2022). Previous research has shown that Fc addition can increase the SPCE detected current density by 136.4 μ A (Wu *et al.*, 2022), compared to the addition of bismuth (62.65 μ A), gold (96.33 μ A), and bare SPCE (42.48 μ A) (Tang *et al.*, 2017). Our previous research also found an increased electrochemical performance for Cu²⁺ analytic electrodes when screen-printed activated carbon from bagasse was modified with ferrocene (Rahmawati *et al.*, 2023). A ferrocene modification also increases the electrochemical performance of SPCE from coconut shell for Pb²⁺ detection by a Limit of Detection (LOD) of 0.35 mM and a consistent result under 10% interference by the presence of other ions (Heliani *et al.*, 2024).

Furthermore, this paper discusses the potential use of the Fc modified-SPCE prepared from coconut shells to detect Cobalt, Co²⁺, and ions. It is important to investigate whether the SPCE from coconut shells can detect some ions by providing different onset anodic and cathodic potentials and different peak positions. Therefore, this research investigated the voltage range of measurement of Co²⁺, the effect of scan rate (mV/s), the onset potential consistency for a various Co²⁺ concentration, and the LoD of this modified Fc-SPCE for Co²⁺ detection.

RESEARCH METHODS

This research used commercial charcoal procured from charcoal producers (Klaten, Central Java, Indonesia). All reagents used were analytical grade and obtained from Merck and Sigma Aldrich. Meanwhile, N-Methyl-2-Pyrrolidinone (NMP) (p.a.), Poly(vinylidene) Fluoride (PVDF) (p.a.), and Acetylene Black (AB) obtained from KGC Saintifik, Indonesia.

The surface morphology and elemental contents were determined using Scanning Electron Microscopy with energy-dispersive X-ray spectroscopy (SEM/EDX) (Hitachi FlexSEM 100). The vibration of functional groups was determined using Fourier-transform Infrared spectroscopy (FTIR) (Shimadzu IR Prestige-2) at 4000 – 400 cm⁻¹ wavenumber. The specific diffraction patterns were determined using X-ray diffraction (XRD) (Rigaku Minifex 600 Cu/K α) at 10° – 60° 2 θ . The Structural properties at the nanometric scale were determined using Raman Spectroscopy (RAMAN iHR320 HORIBA). Meanwhile, the surface area, pore volume, and pore distribution were determined using a Surface Area Analyzer (SAA) (Quantachrome NOVA Touch 4LX) through adsorption-desorption of N₂ gas at 77 K and relative pressure.

Activation of Coconut Shell Carbon

The charcoal was crushed with mortar and pestle into powder and was sieved at 100 mesh. The 100 mesh charcoal powder was then soaked while stirred in distilled water for 1 hour. The distilled water was then decanted and the carbon residue dried at 60°C for 3 hours. The resulting powder was signed as the leached carbon (Char) and analyzed by XRD, FTIR, SAA, and Raman. The following procedure was the activation, in which 25 grams of char was poured into 100 ml of 0.01 M NaOH solution (1 gram: 4 mL ratio) (Song *et al.*, 2011) and heated at 85 °C for 2 hours under stirred conditions (Sujiono *et al.*, 2022). The solution was then neutralized by dropping 0.1 M HCl solution under stirring conditions. The solution was then stored overnight until a residue formed and could be decanted. Afterward, the residue was dried for 3 hours at 130 °C (Sujiono *et al.*, 2022). The resulting powder was signed as the activated carbon (Ac) and weighted to calculate mass degradation and % activation yield by applying Equation (1). The weight of Ac refers to the final weight after activation (g), and the weight of char refers to the weight of the leached coconut shell carbon to be activated (g). The activated carbon was then analyzed by SEM/EDX, FTIR, XRD, SAA, and Raman.

$$\% \text{ yield} = \frac{\text{weight of Ac}}{\text{weight of Char}} \times 100 \quad (1)$$

Preparation of Screen-Printed Carbon Electrode (SPCE)

Carbon slurry was made by mixing Ac, conductive agent (AB), and binder (PVDF) with a mass ratio of 7:2:1. Meanwhile, NMP was used as a dispersant (Huang *et al.*, 2021). The carbon slurry was stirred at room temperature

until homogeneous. The slurry was then cast on a SPCE pattern that was printed by the Epson L210 series on PVC paper. The SPCE pattern is shown in Figure 1(a). The casted SPCE was then attached to a vacuum casting machine and then dried at 50 °C under vacuum conditions for 5 min, followed by heating in a vacuum oven to obtain good adhesion between the activated carbon ink with the PVC substrate (Wahyuni *et al.*, 2021). After drying in a vacuum oven, the reference part was painted with silver paste, as shown by Figure 1(b), and Fc was added to the working electrode (WE). The three parts of the electrodes were then applied with paraffin liquid to prevent a short contact, as shown in Figure 1(c) (Rahmawati *et al.*, 2023). The result was then used in electrochemical analysis of Co(II) with cyclic voltammetry.

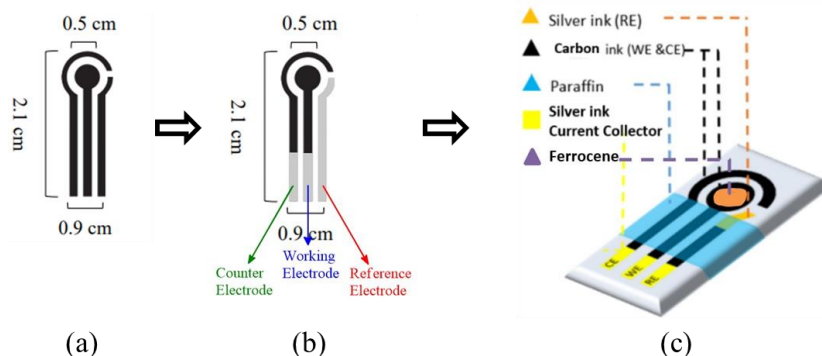


Figure 1. (a) Geometric of SPCE on PVC Paper, (b) three electrodes of SPCE, (c) and scheme of SPCE.

Electrochemical Test

A Cyclic Voltammetry (CV) test was conducted with CorrTest Electrochemical Workstation CS150 with Co (II) solution as an analyte to know the performance of the prepared SPCE. The prepared SPCE was attached to the electrode socket and dipped into the CoCl₂ solution. The SPCE socket and solution chamber were assembled in an argon glove box (CY-VGB-1 with UHP Argon gas) to prevent oxygen disturbance during measurement. The assembled SPCE and the analyte solution are described in Figure 2. To check the optimum Fc percentage, the SPCE, modified by 10%, 20%, and 30% Fc, were applied to 4×10⁻⁶ M CoCl₂ solution and objected to CV analysis at -1.5 to 1.5 V vs Ag/AgCl at 10 mV s⁻¹ scan rate. The optimum Fc content was then applied further to investigate the optimum scan rate and SPCE limit detection. The SPCE with optimum Fc was then used to 2×10⁻⁴ M CoCl₂ solution and objected to CV analysis at 2.5 to -2.5 V vs. Ag/AgCl with various scan rates of 2, 3, and 5 mV s⁻¹. The optimum scan rate and Fc content were then applied further to investigate SPCE limit detection by conducting CV analysis at 2.5 to -2.5 V vs Ag/AgCl with various analyte (CoCl₂ solution) concentrations of 5×10⁻⁵, 2×10⁻⁴, 4×10⁻⁴, and 8×10⁻⁴ M.

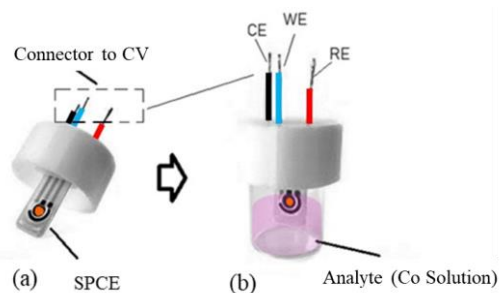


Figure 2. (a) The SPCE socket and (b) the assembled socket with the analyte solution chamber.

RESULTS AND DISCUSSION

Characterization of The Activated Carbon

The carbon leaching before activation resulted in char with an 87.1% yield. Meanwhile, the activation process produced activated carbon, Ac, at 75.39% yield. The weight loss after activation originated from the degradation of cellulose, hemicellulose, lignin, and unstable components in coconut shells (Wang *et al.*, 2013). The char and Ac optical images are shown in Figure 3. The Ac morphology was then tested using SEM, and the result images are shown in Figure 4.

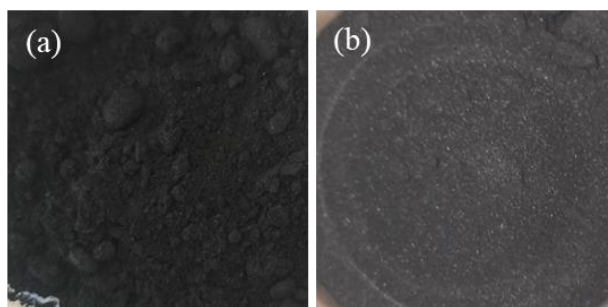


Figure 3. Optical image of (a) Char and (b) Ac.

Figures 4 a, b, c, and d show the microscopic surface of dry bagasse at various magnifications. From Figure 4, it can be seen that Ac has a chip-like morphology, which consists of micro holes with a size $<5 \mu\text{m}$, indicating the porous surface of the Ac. EDX analysis confirmed that the Ac consists of C, O, and Si. The weight percent of each element is listed in Table 1, which shows a similarity with previous research (Sujiono *et al.*, 2022). The presence of Na could be a consequence of alkaline treatment (Rahmawati *et al.*, 2023). Moreover, the presence of N, O, Na, Mg, and K in carbon is from the soil's micronutrients naturally available in coconut shells (Sujiono *et al.*, 2022). Meanwhile, the presence of Al, Fe, and S is probably caused by carbon impurities. A high C content within Ac ensures that coconut shell is a promising raw material for activated carbon production.

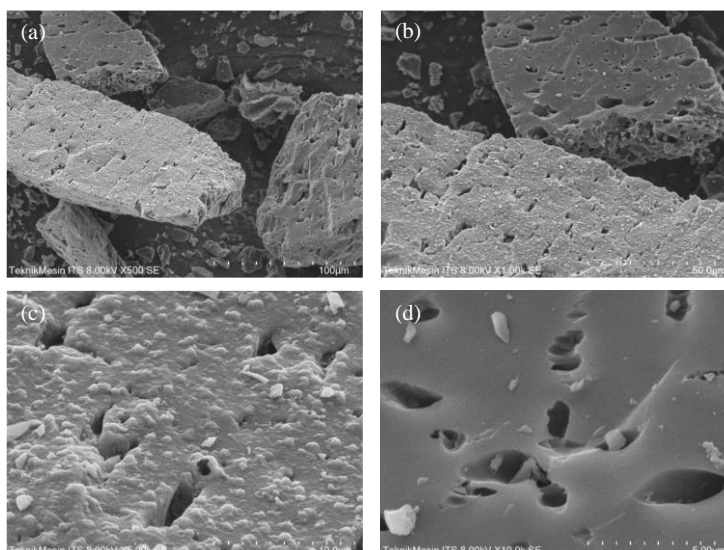


Figure 4. SEM analysis of Ac at different magnifications.

Table 1. EDX Analysis of Ac.

Elements	Percentage (%)
C	61.70
N	13.45
O	17.04
Na	1.24
Mg	0.74
Al	0.83
Si	0.88
S	2.12
K	1.01
Fe	1.08

FTIR analysis of Char and Ac found some spectrum depicted in Figure 5. A broad peak at 3421–3530 cm^{-1} indicates O–H *stretching* from a hydroxyl group and phenolic group within cellulose molecule (Rahmawati *et al.*, 2023; Sujiono *et al.*, 2022). A peak at 1733–2354 cm^{-1} is C=O *stretching*, which comes from carboxylic acids (Sujiono *et al.*, 2022), aldehydes, and ketones from cellulose, hemicellulose, and lignin (Rahmawati *et al.*, 2023). However, the C=O *stretching* peak can only be found in char and isn't present in Ac's FTIR spectrum. The peaks at 1745 cm^{-1} (Char) and 1548 cm^{-1} (Ac) belong to the C=C *aromatic* bond (Cazetta *et al.*, 2011; Shrestha, 2016). The C–O *stretching* peak can be found at 1054 cm^{-1} (Char) and 1037 cm^{-1} (Ac), which come from glucoside bonds from cellulose, hemicellulose, and lignin (Rahmawati *et al.*, 2023). Furthermore, the Si–O *bending* peak can be found in both Char and Ac's spectra at 806 cm^{-1} and 807 cm^{-1} , indicating silicate's presence in coconut shells (Rahmawati *et al.*, 2023). The char and Ac spectrums also show the presence of an O–H *out-of-plane* group indicated by a peak at 580 cm^{-1} (Cazetta *et al.*, 2011). The FTIR analysis shows that the activation treatment decreased the intensity of O–H *stretching* and C=C *aromatic* peak and removed the C=O *stretching* group.

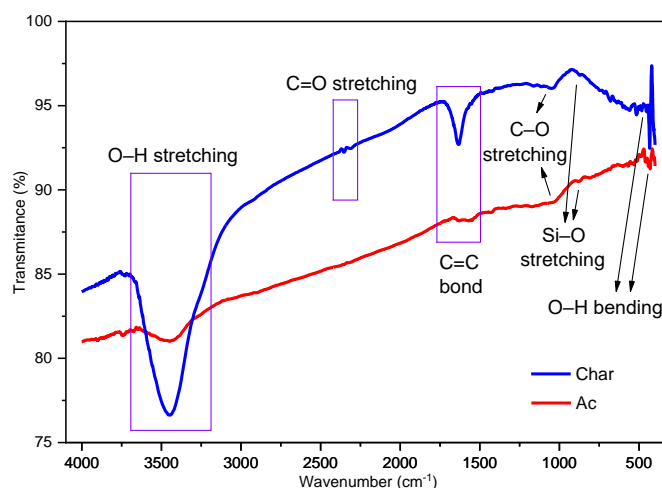


Figure 5. FTIR analysis of Char and Ac at 4000–400 cm^{-1} wavenumber.

The XRD pattern of both carbons shows a diffraction pattern with a broad peak lying between 25° and 43° (Figure 6). The pattern is close to amorphous carbon prepared by previous research (Abdullah *et al.*, 2018). The XRD patterns fit with standard diffraction of amorphous carbon, JCPDS 41-1487. However, a peak at 2 θ 15°, which appears in char, is unavailable in the Ac diffraction pattern. The peak refers to SiO₂, confirmed by JCPDS 32-0993. Activation treatment successfully removed SiO₂ content from char. Furthermore, Rahmawati *et al.* (2023) stated that the SiO₂ removal was a consequence of the usage of NaOH in the carbon treatment. The removal of the SiO₂ reaction was shown by Reaction 1.

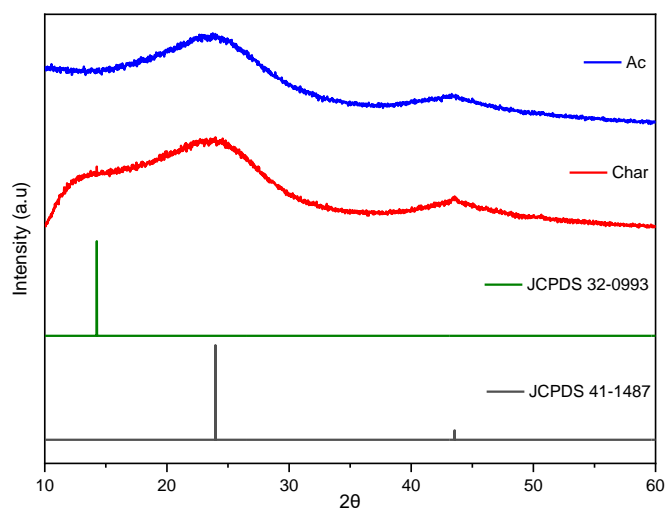


Figure 6. XRD analysis of Char and Ac at 10° – 60° 2 θ .

Surface area analysis of char and Ac shows that the activation treatment significantly increased the surface area, pore volume, and average pore size (Table 2). After the activation treatment, the surface area increases from 46.598 m² g⁻¹ (char) to 154.612 m² g⁻¹ (Ac). The total pore volume also increases from 0.0327 cm³ g⁻¹ for char to 0.109 cm³ g⁻¹ for Ac, confirmed by BET calculation as listed in Table 2. The average pore size increases from 1.406 nm (char) to 1.42 nm (Ac). Both carbon pore radius was categorized as micropores (size < 2 nm), similar to the previous research (Sujiono *et al.*, 2022). The isotherm graphs (Figure 7) show that activation treatment also increases the total volume of N₂ adsorbed by Ac. According to Figure 7, the adsorption isotherms of both carbons follow type II, like previous research (Sujiono *et al.*, 2022). However, the isotherm curves are not fully closed, which may be caused by the strong adsorption of N₂ molecules to the carbon surface, which were hard to desorb or need more equilibrium time to be released entirely (Rahmawati *et al.*, 2023).

Table 2. SAA Analysis of Char and Ac.

Parameter	Char	Ac
BET surface area (m ² g ⁻¹)	46.598	154.612
Average pore size (nm)	1.406	1.42
Pore volume (cm ³ g ⁻¹)	0.0327	0.109

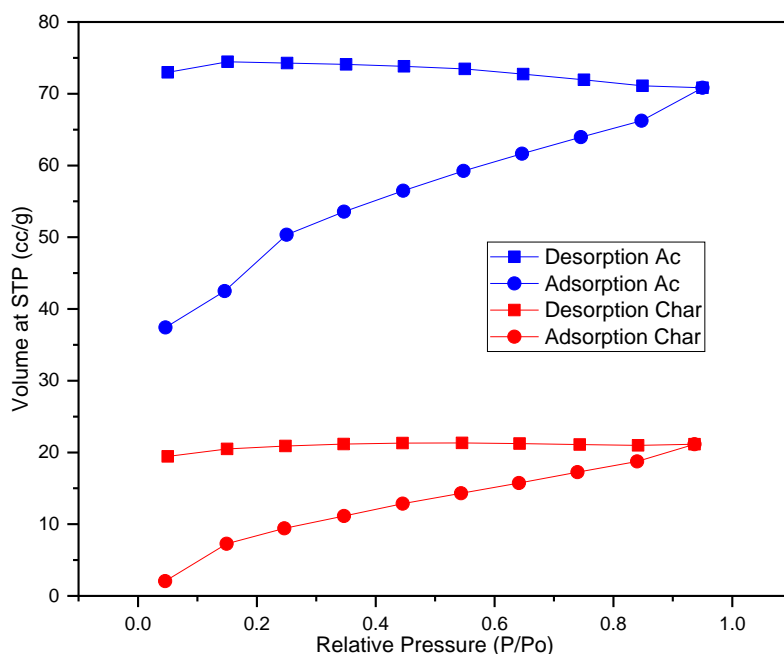


Figure 7. Adsorption–desorption graph of Char and Ac for N₂ gas at 77 K and relative pressure.

Raman spectroscopy analyzed graphitization degree through D and G band ratios. The Raman spectrum, as shown in Figure 8, provides similar patterns of Char and Ac, with two peaks at around 1345 cm⁻¹ (D) and 1600 cm⁻¹ (G) referring to amorphous carbon (Shrestha, 2016). D band appears at 1350 cm⁻¹, indicating vibration of sp³ hybridization of the irregular carbon structure or defect structure. Meanwhile, the G band at around 1600 cm⁻¹ represents graphitized carbon with sp² hybridization. The char's D and G intensity band ratio (I_D/I_G) is 0.83, while Ac has a D and G intensity ratio of 0.84. A higher I_D/I_G ratio value indicates more defects available within the carbon structure and represents the amorphousness of the carbon (Mopoung and Dejang, 2021).

An impedance measurement was conducted to understand the electronic properties of the prepared Ac. The Nyquist plot of impedance is depicted in Figure 9. ZView fitting proceeded well by applying the R-L network as shown by the inserted scheme within Figure 9. The fitting result found resistant R of 1.56 Ω, resulting in conductivity of 5.89 × 10⁻¹ S cm⁻¹ by applying Equation (1) with the distance between two active electrodes, *l* of 0.739 cm, and area of the active electrode, A, 0.804 cm². The conductivity is higher than previous research on coconut shell carbon preparation, i.e., 2.36 × 10⁻⁸ S cm⁻¹ (Azari *et al.*, 2021).

$$\sigma = \frac{1}{R} \frac{l}{A} \quad (1)$$

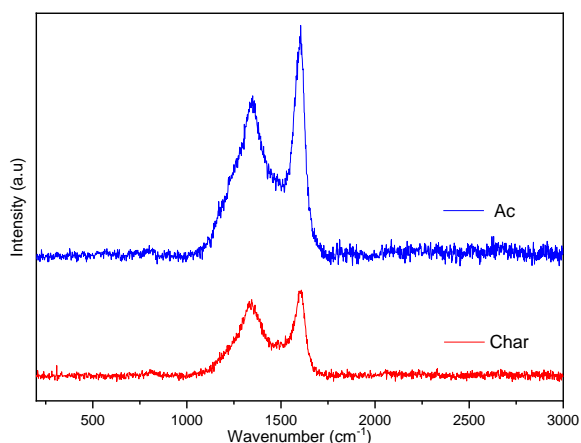


Figure 8. Raman spectrum of char and Ac.

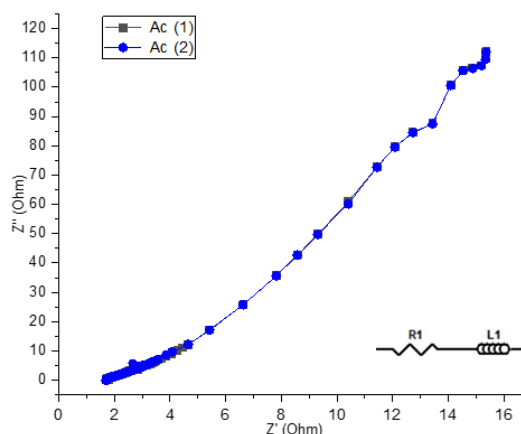


Figure 9. Nyquist plot of char and the used R-L network.

Electrochemical Tests of the SPCE

CV analysis to Co (II) solution with the prepared-SPCE from Ac or SPCE-Ac was done at various FC content of 10%, 20%, and 30%. The result shows that SPCE 10% Fc has the highest current density of 0.7545 mA/cm², as shown in [Figure 10](#). It seems that too much Fc even reduces the electrode performance because the modifier can blockage the pores and reduces the conductivity of the electrode ([Mossfika et al., 2020](#)). SPCE 10% Fc was then further investigated to understand the scan rate factor. The results are described in [Figure 11](#), which shows that 2 mVs⁻¹ provide more distinctive anodic and cathodic peaks. However, the voltammograms provide similar anodic and cathodic onset potential, i.e., 0.2 V vs. Ag/AgCl at 2, 3, and 5 mVs⁻¹, confirming the stable performance of SPCE under different scan rates ([Figure 11](#)).

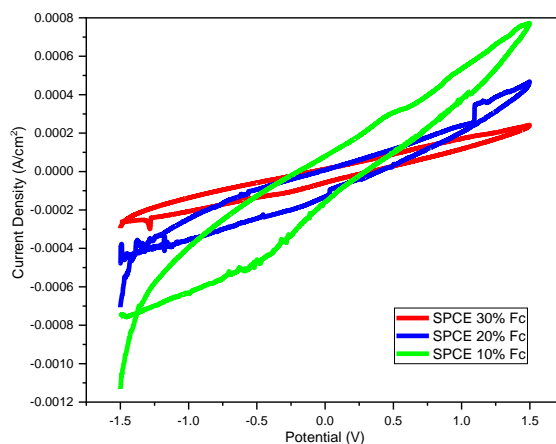


Figure 10. Cyclic voltammogram of the ferrocene percentage optimization.

The LOD of SPCE 10% Fc was tested with various concentrations of CoCl₂ analyte. The result is shown in [Figure 12](#), where the voltammogram response of cobalt reduction-oxidation revealed that the anodic and cathodic peaks became more distinctive as the concentration of CoCl₂ solutions increased. Based on the standard deviation calculation in [Equation 2](#), limit of detection (LoD) was then determined by using [Equation 3](#), in which SD refers to standard deviation, x_i refers to data union value, \bar{x} refers to the data average, n refers to lots of the data, $n-1$ refers to the degrees of freedom (df), m refers to the slope of the calibration curve plot of anodic peak current versus cobalt(II) concentration, and LoD refers to the detection limit ([Heliani et al., 2024](#); [Rahmawati et al., 2023](#)).

$$SD = \sqrt{\frac{\sum_{i=1}^n (x_i - \bar{x})^2}{n-1}} \quad (2)$$

$$LoD = \frac{3 \times SD}{m} \quad (3)$$

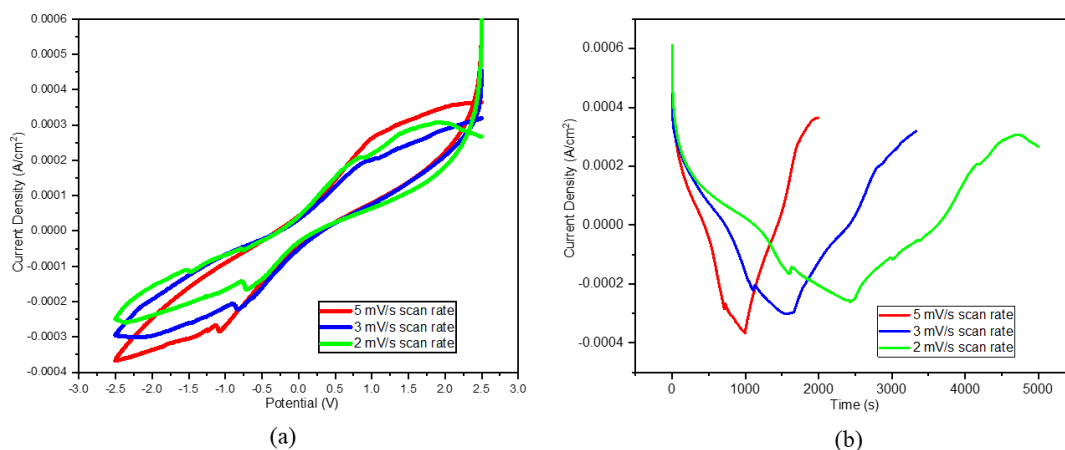


Figure 11. Cyclic voltammogram of (a) SPCE at various scan rates and (b) SPCE at various scan rates and experiment times.

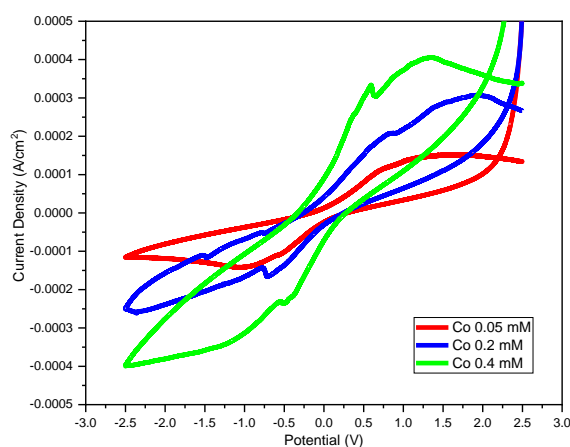


Figure 12. Cyclic voltammogram of SPCE at various analyte concentrations (Co solution).

The LOD of SPCE10%Fc is $0.224 \text{ mmol L}^{-1}$. The result is compared with other published research works listed in Table 3. It shows that the prepared SPCE 10%Fc in this research provides a lower LoD than the others, indicating higher sensitivity. Furthermore, this research confirms that coconut shell char is a promising raw material for SPCE production.

Table 3. Some various SPCE and GCE for CV analysis.

Electrodes	Analytes or Samples	Analytical Characteristics	References
Graphite Ink Combination with Polystyrene	Uric Acid	L.R: 0.01–0.08 mM LOD: 0.0019 mM	(Wahyuni <i>et al.</i> , 2021) (Wahyuni <i>et al.</i> , 2021)
Polyurethane-LiClO ₄	Histamine	L.R: 0.015–1 mM LOD: 0.035 mM	(Munir <i>et al.</i> , 2022)
Patterned waxed paper screen-printed with silver ink	Chloride/serum, sweat	L.R: 10–200 mM LOD: 1 mM	(Cinti <i>et al.</i> , 2018)
Au-MoA-D4-GlutOX	Glutamate	L.R: 5–25 mM LOD: 1.9 mM	(Urbanowicz <i>et al.</i> , 2023)
tetra-tert-butyl phthalocyanine (PcH ₂ -tBu)/Carbon (C)	Volatiles Fatty Acids (VFAs)	L.R: 100–400 mM LOD: 25.77 mM	(Ndiaye <i>et al.</i> , 2016)
SPCE 10% Fc	Cobalt ions	L.R: 0.05–0.4 mM LOD: 0.244 mM	This Work

CONCLUSION

This research found that activation treatment to coconut shell char increases the surface area from 46.598 m²/g to 154.612 m²/g for Char and Ac, respectively. The activation step also removed SiO₂ content, allowing the activated carbon, Ac, to provide a high conductivity of 5.89×10⁻¹ S cm⁻¹. The conductivity value ensuring Ac is a good material for electrode production. The electrode, SPCE from Ac with 10%Fc as a modifier, shows a good performance in Co(II) analysis with a LoD of 0.224 mM. This study confirms that coconut shell char is a potential raw material for SPCE production. The coconut shell's high abundance and renewability will support sustainable SPCE production without dependence on fossil coals.

CONFLICT OF INTEREST

There is no conflict of interest in this article.

AUTHOR CONTRIBUTION

MF: data analysis and manuscript drafting; EH: supervision and manuscript review; AM: supervision, data analysis, and editing; MAM: manuscript review and editing; FR: research coordination, supervision, conceptualization, and funding acquisition.

ACKNOWLEDGEMENTS

The authors acknowledge Sebelas Maret University for funding this research under PUT-UNS scheme, contract number 228/UN27.22/PT.01.03/2023.

REFERENCES

- Abdullah, N.H., Inu, I., Razab, Abdul, M.K.A., Noor, A., Zauddin, M., Che, N.A., Rasat, M.S., Mat Amin, Mohamad Faiz Mohd Abdullah, W.N., and Wan Shukri, Nurasmah Mohd Halim, A.Z., 2018. Effect of Acidic and Alkaline Treatments to Methylene Blue Adsorption from Aqueous Solution by Coconut Shell Activated Carbon. *International Journal of Current Research in Science, Engineering & Technology*, 1, 319. <https://doi.org/10.30967/ijcrset.1.S1.2018.319-324>.
- Azari, B.L.H., Wicaksono, T., Damayanti, J.F., and Azari, D.F.H., 2021. The Study of The Electrical Conductivity and Activation Energy on Conductive Polymer Materials. *Computational And Experimental Research In Materials And Renewable Energy*, 4, 71. <https://doi.org/10.19184/cerimre.v4i2.28371>.
- Cazetta, A.L., Vargas, A.M.M., Nogami, E.M., Kunita, M.H., Guilherme, M.R., Martins, A.C., Silva, T.L., Moraes, J.C.G., and Almeida, V.C., 2011. NaOH-Activated Carbon of High Surface Area Produced from Coconut Shell: Kinetics and Equilibrium Studies from the Methylene Blue Adsorption. *Chemical Engineering Journal*, 174, 117–125. <https://doi.org/10.1016/j.cej.2011.08.058>.
- Cinti, S., Fiore, L., Massoud, R., Cortese, C., Moscone, D., Palleschi, G., and Arduini, F., 2018. Low-Cost and Reagent-Free Paper-Based Device to Detect Chloride Ions in Serum and Sweat. *Talanta*, 179, 186–192. <https://doi.org/10.1016/j.talanta.2017.10.030>.
- Ferlazzo, A., Bressi, V., Espro, C., Iannazzo, D., Piperopoulos, E., and Neri, G., 2023. Electrochemical Determination of Nitrites and Sulfites by Using Waste-Derived Nanobiochar. *Journal of Electroanalytical Chemistry*, 928, 117071. <https://doi.org/10.1016/j.jelechem.2022.117071>.
- Heliani, K.R., Rahmawati, F., and Wijayanta, A.T., 2024. Screen Printed Carbon Electrode from Coconut Shell Char for Lead Ions Detection. *International Journal of Renewable Energy Development*, 13, 19–30. <https://doi.org/10.14710/ijred.2024.57679>.
- Hu, L., Zhou, X., Li, J., Bai, T., Tang, J., Zhou, T., and Cui, Q., 2018. Ferrocene/Graphene Modified Glassy Carbon Electrode for Chloromycetin Detection. *International Journal of Electrochemical Science*, 13, 396–409. <https://doi.org/10.20964/2018.01.09>.
- Huang, L., Wang, S., Zhang, Y., Huang, X.H., Peng, J.J., and Yang, F., 2021. Preparation of a N-P Co-Doped Waste Cotton Fabric-Based Activated Carbon for Supercapacitor Electrodes. *Xinxing Tan Cailiao/New Carbon Materials*, 36, 1128–1137. [https://doi.org/10.1016/S1872-5805\(21\)60054-9](https://doi.org/10.1016/S1872-5805(21)60054-9).
- Kuan-Ching Lee, Mitchell Shyan Wei Lim, Zhong-Yun Hong, S.C.G.-T.P. and C.-M.H., 2021. Coconut Shell-Derived Activated Carbon for High-Performance. *Energies*, 14, 4546.
- Ma, F., Li, X., Li, Y., Feng, Y., and Ye, B.-C., 2022. High current flux electrochemical sensor based on nickel-iron bimetal pyrolytic carbon material of paper waste pulp for clenbuterol detection. *Talanta*, 250, 123756. <https://doi.org/10.1016/j.talanta.2022.123756>.

- Mopoung, S., and Dejang, N., 2021. Activated Carbon Preparation from Eucalyptus Wood Chips Using Continuous Carbonization-Steam Activation Process in a Batch Intermittent Rotary Kiln. *Scientific Reports*, 11, 13948. <https://doi.org/10.1038/s41598-021-93249-x>.
- Mossfika, E., Syukri, S., and Aziz, H., 2020. Preparation of Activated Carbon from Tea Waste by NaOH Activation as A Supercapacitor Material. *Journal of Aceh Physics Society*, 9, 42–47. <https://doi.org/10.24815/jacps.v9i2.15905>.
- Munir, M.A., Badri, K.H., Heng, L.Y., Inayatullah, A., Nurinda, E., Estiningsih, D., Fatmawati, A., Aprilia, V., and Syafitri, N., 2022. The Application of Polyurethane-LiClO₄ to Modify Screen-Printed Electrodes Analyzing Histamine in Mackerel Using a Voltammetric Approach. *ACS Omega*, 7, 5982–5991. <https://doi.org/10.1021/acsomega.1c06295>.
- Ndiaye, A.L., Delile, S., Brunet, J., Varenne, C., and Pauly, A., 2016. Electrochemical Sensors Based on Screen-Printed Electrodes: The Use of Phthalocyanine Derivatives for Application in VFA Detection. *Biosensors*, 6. <https://doi.org/10.3390/bios6030046>.
- Rahmawati, F., Heliani, K.R., Wijayanta, A.T., Zainul, R., Wijaya, K., Miyazaki, T., and Miyawaki, J., 2023. Alkaline Leaching-Carbon from Sugarcane Solid Waste for Screen-Printed Carbon Electrode. *Chemical Papers*. <https://doi.org/10.1007/s11696-023-02712-8>.
- Rahmawati, F., Yuliati, L., Alaih, I.S., and Putri, F.R., 2017. Carbon Rod of Zinc-Carbon Primary Battery Waste as a Substrate for CdS and TiO₂ Photocatalyst Layer for Visible Light Driven Photocatalytic Hydrogen Production. *Journal of Environmental Chemical Engineering*, 5, 2251. <https://doi.org/10.1016/j.jece.2017.04.032>.
- Ridasepri, A.F., Rahmawati, F., Heliani, K.R., Chairunnisa, Miyawaki, J., and Wijayanta, A.T., 2020. Activated Carbon from Bagasse and Its Application for Water Vapor Adsorption. *Evergreen*, 7, 409–416. <https://doi.org/10.5109/4068621>.
- Shrestha, S., 2016. Chemical, Structural and Elemental Characterization of Biosorbents Using FE-SEM, SEM-EDX, XRD/XRPD and ATR-FTIR Techniques. *Journal of Chemical Engineering & Process Technology*, 7. <https://doi.org/10.4172/2157-7048.1000295>.
- Song, X., Gunawan, P., Jiang, R., Leong, S.S.J., Wang, K., and Xu, R., 2011. Surface Activated Carbon Nanospheres for Fast Adsorption of Silver Ions from Aqueous Solutions. *Journal of Hazardous Materials*, 194, 162–168. <https://doi.org/10.1016/J.JHAZMAT.2011.07.076>.
- Sujiono, E. H., Zabrian, D., Zurnansyah, Mulyati, Zharvan, V., Samnur, and Humairah, N.A., 2022. Fabrication and Characterization of Coconut Shell Activated Carbon Using Variation Chemical Activation for Wastewater Treatment Application. *Results in Chemistry*, 4, 100291. <https://doi.org/10.1016/j.rechem.2022.100291>.
- Tang, H., Wang, M., Lu, T., and Pan, L., 2017. Porous Carbon Spheres as Anode Materials for Sodium-Ion Batteries with High Capacity and Long Cycling Life. *Ceramics International*, 43, 4475–4482. <https://doi.org/10.1016/j.ceramint.2016.12.098>.
- Trisunaryanti, W., Wijaya, K., Triyono, T., Wahyuningtyas, N., Utami, S.P., and Larasati, S., 2022. Characteristics of Coconut Shell-Based Activated Carbon as Ni and Pt Catalyst Supports for Hydrotreating Calophyllum Inophyllum Oil into Hydrocarbon-Based Biofuel. *Journal of Environmental Chemical Engineering*, 10, 108209. <https://doi.org/10.1016/j.jece.2022.108209>.
- Urbanowicz, M., Sadowska, K., Lemieszek, B., Paziewska-Nowak, A., Słodatowska, A., Dawgul, M., and Pijanowska, D.G., 2023. Effect of Dendrimer-Based Interlayers for Enzyme Immobilization on a Model Electrochemical Sensing System for Glutamate. *Bioelectrochemistry*, 152. <https://doi.org/10.1016/j.bioelechem.2023.108407>.
- Wahyuni, W.T., Putra, B.R., Heryanto, R., Rohaeti, E., Yanto, D.H.Y., and Fauzi, A., 2021. A Simple Approach to Fabricate a Screen-Printed Electrode and Its Application for Uric Acid Detection. *International Journal of Electrochemical Science*, 16, 1–14. <https://doi.org/10.20964/2021.02.36>.
- Wang, G., Qian, B., Dong, Q., Yang, J., Zhao, Z., and Qiu, J., 2013. Highly Mesoporous Activated Carbon Electrode for Capacitive Deionization. *Separation and Purification Technology*, 103, 216–221. <https://doi.org/10.1016/j.seppur.2012.10.041>.
- Wu, B., Yeasmin, S., Liu, Y., and Cheng, L.J., 2022. Ferrocene-Grafted Carbon Nanotubes for Sensitive Non-Enzymatic Electrochemical Detection of Hydrogen Peroxide. *Journal of Electroanalytical Chemistry*, 908. <https://doi.org/10.1016/j.jelechem.2022.116101>.